

A statistical model of aggregate fragmentation

F Spahn^{1,4}, E Vieira Neto², A H F Guimarães², A N Gorban³ and N V Brilliantov³

¹ Institute of Physics, University of Potsdam, Am Neuen Palais 10, D-14469 Potsdam, Germany

² Grupo de Dinâmica Orbital e Planetologia, UNESP, São Paulo, Brazil

³ Department of Mathematics, University of Leicester, Leicester LE1 7RH, UK

E-mail: fspahn@agnld.uni-potsdam.de

Received 16 September 2013, revised 4 December 2013

Accepted for publication 12 December 2013

Published 17 January 2014

New Journal of Physics **16** (2014) 013031

doi:[10.1088/1367-2630/16/1/013031](https://doi.org/10.1088/1367-2630/16/1/013031)

Abstract

A statistical model of fragmentation of aggregates is proposed, based on the stochastic propagation of cracks through the body. The propagation rules are formulated on a lattice and mimic two important features of the process—a crack moves against the stress gradient while dissipating energy during its growth. We perform numerical simulations of the model for two-dimensional lattice and reveal that the mass distribution for small- and intermediate-size fragments obeys a power law, $F(m) \propto m^{-3/2}$, in agreement with experimental observations. We develop an analytical theory which explains the detected power law and demonstrate that the overall fragment mass distribution in our model agrees qualitatively with that one observed in experiments.

1. Introduction

Fragmentation processes are ubiquitous in nature and play an important role in many industrial processes. Numerous examples range from manufacturing comminution to collision of cosmic bodies in space. Hence, much effort has been devoted to comprehend the nature of fragmentation in different branches of research—geophysics [1, 2], astrophysics [3, 4], engineering [5] and material- [6] or military science [7, 8].

An intriguing common property of fragmentation is a power-law mass distribution of the fragments which seems to be independent of the spatial scale or nature of the parent

⁴ Author to whom any correspondence should be addressed.



Content from this work may be used under the terms of the [Creative Commons Attribution 3.0 licence](https://creativecommons.org/licenses/by/3.0/). Any further distribution of this work must maintain attribution to the author(s) and the title of the work, journal citation and DOI.

bodies: when heavy ions collide with a target, or asteroids suffer a high-speed impact, both produce a power-law size (or charge) distribution of debris. This law has been reported in numerous experimental studies, e.g. [9–17].

The theoretical description of fragmentation is developing along two different lines: one, based on continuum mechanics, another—on the general statistical methods, e.g. [9, 18, 19]. Finite element analysis [20], numerical simulations of agglomerate collisions with smooth particle hydrodynamics (SMH) [21] or discrete element method [14, 17]—these are the current tools to treat continuum mechanical problem of colliding material bodies. Alternatively, statistical methods, as random walk [22] or stochastic simulation of crack-tip trajectories [23] were used to model fractal crack formation and propagation. Furthermore, there were attempts to tackle the problem analytically. In particular, a semi-empirical approach to the physics of catastrophic breakup of cosmic bodies has been developed [24]; similarly, a micro-structural approach has been adopted [25] to model the fracture generation and propagation in concrete.

The observed universality of the fragmentation law for the objects, drastically different in material properties and dimension, most probably implies a common physical principle inherent to all fragmentation processes [26]. Moreover, it is reasonable to assume that this principle is of statistical nature. This motivates the analysis of a model which, being very simple on the microscopic level, reflects the most prominent features of the process and adequately represents its statistical properties. In the present study, we propose a novel statistical model for fragmentation of aggregates—macroscopic bodies, comprised of a large amount of smaller macroscopic constituents.

The problem of aggregate fragmentation arises in many areas of science and technology, in particular in planetary science, where the availability of an adequate fragmentation model is crucial for an understanding of the formation and evolution of planetary rings, e.g. [27–29] as well as of planetary or satellite systems [30–32].

We show that our model, based on a few very simple physical rules, reproduces the main aspects of the fragmentation process and gives the power-law distribution for the debris size. Moreover, it qualitatively agrees with the experimental data. We perform numerical simulations and develop a simple analytical theory, which explains the observed power-law distribution for the fragments in the case of a two-dimensional (2D) aggregate. Our exclusive focus on adhesive aggregates points at astrophysical applications of our modeling: e.g. the dynamics of dense (granular) planetary rings or even scenarios of formation of planets in circum-stellar gas-aggregate discs.

2. Fragmentation model

We consider aggregates, which are not too large so that gravitation forces can safely be neglected [33], and assume the aggregates' constituents are kept together by the adhesive bonds. These are significantly weaker than the forces attributed to chemical bonds so that the formation of cracks—caused by direct collisions between aggregates—occurs only along the adhesive–dissipative contacts *between* and not *inside* constituents. Hence, the fragmentation processes inside an aggregate considered here are controlled by bulk stresses formed by a network of dissipative, adhesive bonds—which are much weaker than stresses inside breaking solid bodies. Such weak stresses and the dissipation related to dynamical propagation of the bond breakage-chain frustrate the interaction between nearby cracks, which can occur during

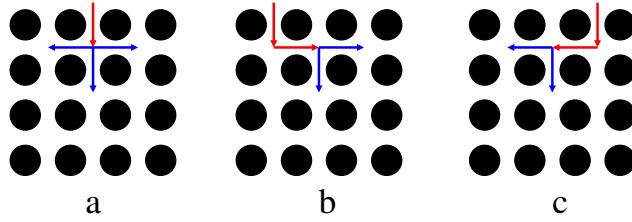


Figure 1. A model aggregate is composed of $l \times l$ identical particles on a square lattice. To break a bond between particles the energy E_b is needed. A crack propagates either away from the loaded surface (vertically down on the plots), against the stress gradient, or laterally, but never along the gradient. All possible directions have equal probability. In the case (a) there exist three allowed directions, each with the probability $p_3 = 1/3$: one away from the surface and two lateral directions. In the cases (b) and (c) only two directions with the probability $p_2 = 1/2$ are possible, since the crack can not move back or ‘uphill’ the load.

a fast fracture of quite elastic solids. Because of this reasoning and for the sake of simplicity, crack–crack interactions as well as branching of cracks are neglected in our model.

For the sake of simplicity, we assume the aggregates to consist of uniform constituents—all of the same size and material. Then to break any adhesive contact, the amount of energy, equal to E_b , is required; to destroy simultaneously n bonds one needs n -times larger energy, nE_b . The quantity E_b depends on the particles size, their surface tension and material parameters, e.g. [34]. To simplify further the problem, we consider its 2D version and assume that the spherical constituents form a square lattice, figure 1.

In a collision between aggregates, which causes their fragmentation, the energy of the relative motion E_{coll} is transformed into the surface energy of broken bonds and the kinetic energy of debris. For the moment, we will ignore the latter part of the energy and explicitly consider just the former one. Therefore, the problem of fragmentation in our model is essentially reduced to the problem of distribution of the energy E_{coll} among the broken adhesive bonds.

Next, we assume the bonds being destroyed due to a stochastic propagation of the cracks. Namely, we adopt the following rules for the crack growth. (i) A crack originates on the surface at the impact site, where the maximum stress is expected. It propagates (in average) away from the surface against the stress gradient, that is, ‘downhill’ the load, and never ‘uphill’. (ii) At each time-step the crack elongates by a single neighboring bond, consuming the energy E_b , while the crack tip performs a random walk with the direction randomly chosen among two or three possible ones, as explained in figure 1. (iii) The propagation of a certain crack terminates if its tip arrives at the surface, or meets another crack. When a crack terminates and the rest-energy allows for further bond breaking, a new crack is initiated randomly on the surface of the aggregate, or bifurcates from another crack. (iv) A mechanism limiting a total crack energy is introduced. This is because crack generation and propagation needs a sufficient load gradient which decreases with distance from the impact site. Thus, we assume that if the energy assigned to a crack, chosen randomly between zero and a maximum E_{cross} , is exhausted, the crack stops and another one is created instead. We called this ‘crossing factor’. (v) The breaking process continues as long as the remaining impact energy, $E_{\text{rest}} = E_{\text{coll}} - nE_b$ (n –current number of broken bonds) is sufficient to break further bonds. It terminates whenever the total impact energy E_{coll} is dissipated in cracks.

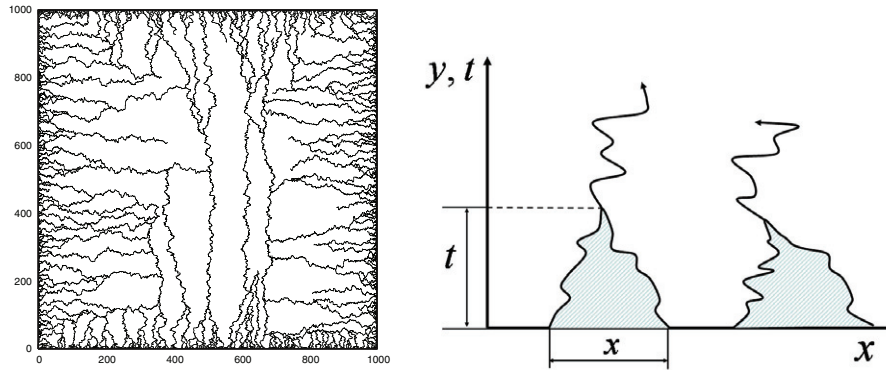


Figure 2. Left panel: a typical fragmentation pattern. The aggregate, composed of one million particles on the 1000×1000 lattice, is broken in 3958 pieces. The total breakage energy is $E_{\text{coll}} = 82\,010E_b$, the crossing-factor is $E_{\text{cross}} = 3000E_b$. Right panel: the fragmentation model may be mapped on the one-dimensional (1D) model of diffusing and annihilating crack-tips. The areas under the crack-tip's trajectories correspond to the fragment masses of the primary fragmentation model.

In figure 2(a) typical fragmentation pattern is shown, which has been obtained by using the above fragmentation rules. In the next section, we analyze the statistical properties of debris.

3. Mass distribution of fragments

We define a fragment as a collection of constituent particles connected by adhesive bonds where a single particle constitutes a mass unit. Hence, for a fragment of m particles we assign the mass m . We have performed numerical experiments, controlling the size of the aggregate, the total energy spent in the process and the crossing factor. To improve the fragments' statistics we perform a large number of runs with the same set of the above parameters.

The left panel of figure 3 shows the fragment mass distribution obtained by 10^4 numerical runs characterizing one and the same aggregate. The distribution (DF) can be approximated by a power law

$$F(m) \propto m^{-\alpha}, \quad m \leq M_F \quad (1)$$

with an approximate slope $\alpha \approx 3/2$ —similar to the results found in 2D egg-shell crushing experiments [14]. The *universal* part of the power-law distribution, which does not depend on the total energy of an impact stretches up to the fraction M_F of the total mass M of the target. This universal part of the power-law distribution refers to small and intermediate fragment sizes, which dominantly originate on the surface of the target. The mass distribution of debris for $m > M_F$ is not universal and depends on the total energy E , which separates the results of the aggregate fragmentation into two classes:

- (i) $E < E_{\text{crit}}$ (partial fragmentation of a body): in this case small and intermediate debris originate exclusively from the surface erosion at fragmentation. The large-mass tail of the fragment distribution is comprised of debris from the core part of the target body. They have masses of the same order as the total mass M and form an excess hump at the right end of the DF (figure 3, left panel).

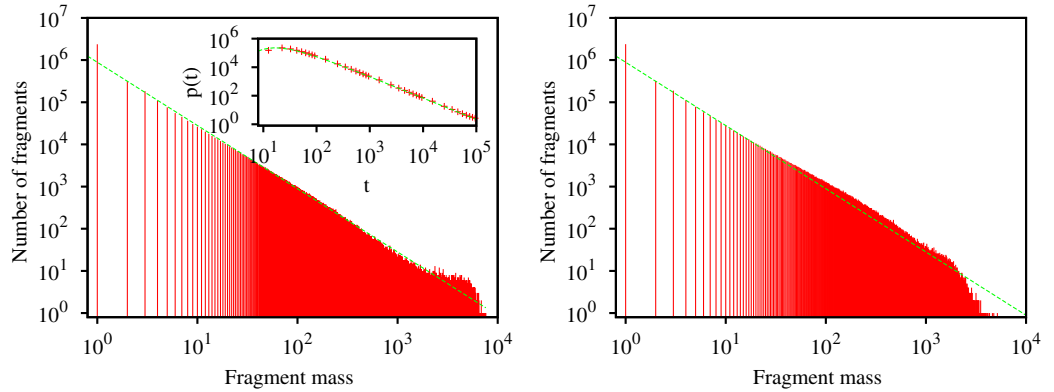


Figure 3. Left panel: fragment mass distribution for a 100×100 lattice matrix with total energy of $E = 4000E_b < E_{\text{crit}}$ and a crossing factor of $200E_b$. The data have been collected for 10 000 runs. The line represents a power-law mass distribution with an exponent $\simeq -3/2$. The inset shows the distribution function $P(x, t) \propto t^{-3/2}$, which gives the probability that two crack-tips, initially separated by distance x , meet at time t (distribution of *first passage times*); it illustrates the affinity of the two models (see the text). Points—numerical data for $x = 20$, line—theory. Right panel: a numerical impact experiment with an impact energy $E > E_{\text{crit}}$.

- (ii) $E > E_{\text{crit}}$ (complete fragmentation of a body): the energy is large enough to break the core of the target body into small and intermediate pieces. In this case there are no fragments of the same order in mass as the total mass M . As a consequence the excess hump disappears and the mass-distribution terminates at smaller masses (figure 3, right panel). Smaller debris are generated on the expense of the large core fragments, changing the distribution of debris in the intermediate range. If the energy is not very large, a part of the DF for small debris remain universal. However, for very large energy the small-size part of the DF will be also affected.

Similar results are obtained when changing the size of the target aggregate. For a given impact energy E , one may either find partly damaged debris (corresponding to case (i)) showing the excess hump for larger fragments provided that the target is large enough—or, alternatively, for smaller targets, finer debris is generated on the expense of the largest fragments (corresponding to case (ii)). In the next section we develop a theory of the fragment mass distribution.

4. Analytical description

4.1. Universal part of the size distribution

The observed power-law fragment size distribution is the result of the robustness of the statistics of the random walk process constituting the basics of our modeling of the fragmentation. This distribution may be explained analytically, if we notice that the proposed fragmentation model may be mapped onto the 1D model of diffusing and annihilating crack-tips. Indeed, the direction normal to the surface, that is, the direction of the most rapid decay of the stress, say axis y (vertically downward in figure 1), may be mapped onto the time axis, since the reverse motion along this axis is forbidden. Then the location of the crack-tips along the lateral direction, say

along axis x (horizontal in figure 1) corresponds to the location of crack-tips on a line. One step along the y axis corresponds to one time step, while one step along the x -axis corresponds to a crack-tip jump on the line (without loss of generality we can assume unit time and space steps).

It is easy to see that the fragmentation model, defined by the rules illustrated in figure 1, is equivalent to the following model: (i) each crack-tip on a line at each time step can remain at the same site with the probability $p_0 = 1/3$, move one site left or right with the probability $p_1 = 1/6$, two sites left or right with $p_2 = 1/12$, etc, k sites left or right with the probability $p_k = 1/(3 \times 2^k)$; note that $p_0 + 2 \sum_k p_k = 1$. (ii) When two crack-tips meet, one of them is destroyed while the other one continues to move with the same rules. (iii) The fragment sizes of the primary fragmentation model is equal to the area confined by the trajectories of the crack-tips and the axis x , as illustrated in figure 2.

First we show that the crack-tips perform a 1D diffusion motion. Indeed, due to the lack of memory, each time step does not depend on the previous one (note that the original problem does have a memory with respect to previous steps). Therefore, the mean square displacement $\langle [\Delta x(t)]^2 \rangle$ is a sum of these quantities for each step, $\langle \Delta^2 \rangle$, where

$$\langle \Delta^2 \rangle = \sum_{l=0}^{\infty} 2 p_l l^2 = \sum_{l=0}^{\infty} \frac{2 l^2}{3 \cdot 2^l} = 4,$$

that is, $\langle [\Delta x(t)]^2 \rangle = 4t = 2Dt$. Hence, we have a diffusive motion with the diffusion coefficient $D = 2$.

Now we compute the distribution of the fragments' areas. These correspond to the areas of the figures on the $x-t$ plane confined by the x -axis and the diffusive trajectories of pairs of crack-tips, which start to move at $t = 0$, and meet at $t > 0$; the initial separation of the crack-tips is x . The area of the figures, that is, the fragment mass scales as $m \propto tx$ (see right part of figure 2). Hence, the mass distribution reads:

$$F(m) \simeq \int dx \int dt \delta(m - \gamma tx) \kappa e^{-\kappa x} P(x, t), \quad (2)$$

where the coefficient γ accounts for the surface mass density of the 2D-aggregate and a geometric factor (1/2 for triangles), which relates a fragment area and its dimensions x and t . The coefficient κ is the line density of crack-tips on the x -axis at the starting time $t = 0$ (i.e. the density of crack tips which start at $y = 0$). A random initial distribution of crack tips corresponds to the Poisson distribution for their initial separation: $\kappa \exp(-\kappa x)$. $P(x, t)$ gives the probability of two diffusing crack-tips, initially separated by distance x , to meet at time t ; where one of the particles is destroyed. $P(x, t)$ may be written as $P(x, t) = \frac{d}{dt} P_{\text{surv}}(x, t)$, where

$$P_{\text{surv}}(x, t) = \int_0^{\infty} \frac{1}{\sqrt{8\pi Dt}} \left(e^{-(y-x)^2/8Dt} - e^{-(y+x)^2/8Dt} \right) dy \quad (3)$$

is the survival probability [35], i.e. that both particles have not been destroyed before time t , provided they started to diffuse at $t = 0$ separated by the distance x . It is obtained from the solution of the diffusion problem with the adsorbing boundary condition for the relative motion of two particles, with the double diffusion coefficient $2D$ (see e.g. [36]).

Indeed the integrand in equation (3) gives the probability distribution of the inter-particle distance y at time t , if the initial separation was x , provided this probability is identically

zero for $y = 0$ (the annihilation condition). Integrating this probability over all distances $y > 0$ gives the survival probability; differentiation of $dP_{\text{surv}}(x, t)/dt$ then yields the probability that the particles meet at time t . Substituting $P(x, t) = x/\sqrt{32Dt^3} \exp(-x^2/8Dt)$ in equation (2), obtained by differentiating equation (3), we finally arrive at the expansion

$$F(m) = A_0 m^{-3/2} + A_1 m^{-5/2} + \dots, \quad (4)$$

where $A_0 = \gamma^{1/2} \Gamma(5/2)/8\kappa^{3/2}$ and generally, $A_l = (-1)^l \Gamma(3l + 5/2)(\gamma/\kappa)^{3l+1/2}/(8\kappa)(4\gamma)^{2l} l!$ is the coefficient corresponding to the power $m^{-(3/2+l)}$. Hence, equation (4) explains the power-law distribution (1) which we have obtained numerically. The above expansion holds, however, not for very small masses, to keep the continuum diffusion approach valid, and not for very large masses, to ignore the effects of energy depletion and finite size effects of the fragmenting pattern.

4.2. Estimates of M_F and the debris critical energy E_{crit}

Here we perform a scaling analysis to estimate the threshold mass M_F and the critical energy E_{crit} . The threshold mass demarcates the universal and non-universal parts of the fragment distribution, while E_{crit} separates two different fragmentation regimes of partial and complete body fragmentation. In the former case the small and intermediate debris originate on the surface of the body, while in the latter one, fragmentation of the core part of the target body contributes to the DF for small and intermediate (practically all remaining) fragments.

To estimate M_F , which mainly makes sense for $E < E_{\text{crit}}$, we notice that the total energy E is distributed among all broken bonds, therefore the energy is equal, up to a constant, to the total length of all cracks L_{cracks} , that is, $E \sim L_{\text{cracks}}$. For the case of partial fragmentation, $E < E_{\text{crit}}$, the total cracks length is mainly accumulated for small and intermediate fragments, that is, for the debris with masses less than M_F . Indeed, the relatively small amount of fragments from the core of the body would not contribute much to L_{cracks} . Therefore we can write

$$L_{\text{cracks}} \sim \int_{m_0}^{M_F} l(m) F(m) dm, \quad (5)$$

where m_0 is the minimal fragment size, $F(m) = A m^{-3/2}$ is the universal distribution function for $m < M_F$ (A is the normalization constant) and $l(m)$ is the perimeter of a fragment of mass m . Again, up to a constant (including the packing density and geometric factor, equal, e.g. to $1/2$ for triangles) we obtain $l(m) \sim m^{1/2}$.

The constant A may be estimated from the normalization of the DF of debris,

$$M = \int_{m_0}^{M_{\text{max}}} F(m) dm \approx \frac{A}{2} \left(m_0^{-1/2} - M_{\text{max}}^{-1/2} \right) \sim A m_0^{-1/2}, \quad (6)$$

where $M_{\text{max}} \gg m_0$ is the mass at which the distribution of debris is terminated. Note that although for $m \sim M_{\text{max}}$ the distribution function deviates from the power law, $\sim m^{-3/2}$, this may affect only quantitatively the normalization constant A , but not its scaling dependence $A \sim m_0^{1/2} M$ on the total mass M , as it follows from equation (6). Hence we obtain using equation (5) and $A \sim M$,

$$\begin{aligned} L_{\text{cracks}} &\sim \int_{m_0}^{M_F} l(m) F(m) dm \sim \int_{m_0}^{M_F} m^{1/2} A m^{-3/2} dm \\ &\sim A \log(M_F/m_0) \sim M \log(M_F/m_0) \end{aligned} \quad (7)$$

and finally, from $E \sim L_{\text{cracks}}$, the following expression of the threshold mass M_F as a function of the total mass M and total energy E :

$$M_F \sim e^{\alpha E/M} \quad (8)$$

with some constant α . To estimate E_{crit} we notice that according to our model a new crack originates on the surface or bifurcates from another crack (see item (iii) of our model in section 2). Hence, if the total energy E is small, the total length of all cracks will be small as compared to the perimeter of the body. The dominant part of the cracks originates in this case on the surface (boundary in 2D) of the target, so that all small and intermediate debris are eroded from the body surface (boundary). Contrarily, if the total energy E is large, the total length of all cracks is comparable or even larger than the perimeter of the fragmenting body. Then, many cracks start in the bulk of the body (bifurcating from the cracks) and give rise to small and intermediate fragments due to the decomposition of the core part of the target. It is reasonable to assume that just at the critical energy E_{crit} the length of all cracks L_{cracks} is equal to the perimeter of the body, which scales as $M^{1/2}$, that is, for the critical energy $E = E_{\text{crit}}$ the condition $L_{\text{cracks}} \sim M^{1/2}$ holds true.

Since at the critical energy the universal distribution up to M_F is not yet violated, one can adopt the estimate (7) for L_{cracks} , which yields for M_F for the case $E = E_{\text{crit}}$:

$$M_F \sim e^{\frac{\beta}{\sqrt{M}}}; \quad \text{for } E = E_{\text{crit}} \quad (9)$$

with some constant β . Using again $E \sim L_{\text{cracks}}$, together with equations (7) and (9) we finally obtain

$$E_{\text{crit}} \sim M \log M_F \sim M \log e^{\frac{\beta}{\sqrt{M}}} \sim \sqrt{M}. \quad (10)$$

Hence the critical energy E_{crit} scales as the surface (perimeter) of the target body. The last conclusion may be also directly obtained from the following simple reasoning: at the critical energy $E = E_{\text{crit}}$ the length of all cracks should be approximately equal to the perimeter of the body, which scales as $M^{1/2}$. Since the total energy is proportional to the total length of all cracks, we obtain, $E_{\text{crit}} \sim M^{1/2}$.

5. Comparison with experiments

So far we have considered the size distribution of fragments which mass is much smaller than the initial mass of the parent body. In this limit the numerically detected and explained power-law distribution coincides with the experimental one [14]. Surprisingly, our model can qualitatively and sometimes even semi-quantitatively reproduce the whole size distribution of fragments in some impact experiments. This is illustrated in figure 4 for the experiments of exploding egg-shells [14], and in figure 5 for the colliding basalt spheres [10]. For the former case our model demonstrates an overall qualitatively correct behavior for $F(m)$, while for the latter case one can achieve a quantitative agreement with the most part of the experimental fragment size distribution.

It is worth noting that the agreement is obtained without any fitting or scaling of our data (still, however, we can vary the total collision energy and the crossing-factor). Moreover, the fact that our simple 2D model can describe the fragmentation statistics for three-dimensional (3D) bodies indicates, that the main ingredients of our model—the diffusive propagation of cracks against the stress gradient and the depletion of energy with the cracks' growth—belong at least to the basic features of fragmentation processes in general.

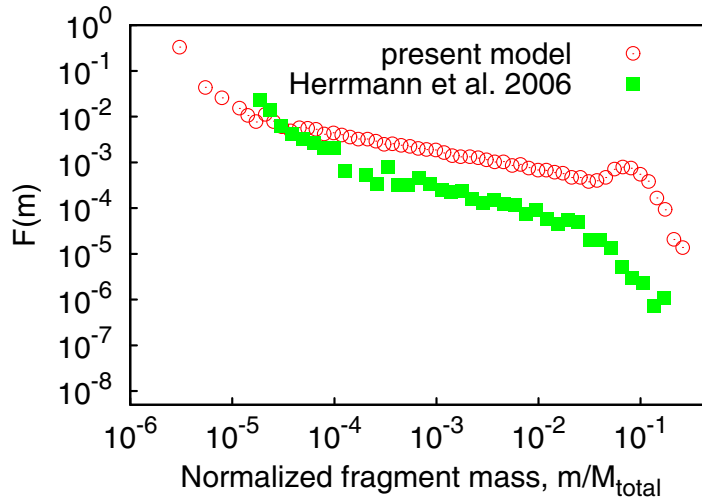


Figure 4. Results of our model (red circles) compared with the experimental data (green squares) of Herrmann *et al* [14]. In simulations we used a 600×600 matrix, the total energy of $E_{\text{coll}} = 40\,000E_b$, the crossing-factor of $E_{\text{cross}} = 3000E_b$ and the number of runs is 200. Note the lack of any fitting or scaling of our data.

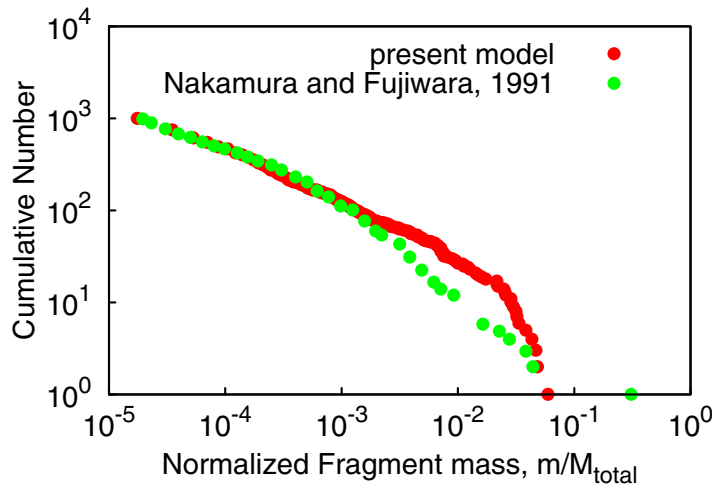


Figure 5. Results of our model (red circles) compared with the experimental data (green circles) of Nakamura and Fujiwara [10]. In simulations we used a 80×80 matrix, the total energy of $E_{\text{coll}} = 1500E_b$, the crossing factor of $E_{\text{cross}} = 100E_b$; the number of runs is 10.

6. Conclusions

We have suggested a simple fragmentation model, based on a lattice random walk of a crack with propagation rules which mimic a real fragmentation process: a crack moves against (or laterally to) the stress gradient and the energy of the crack exhausts along its growth. We have performed numerical simulations of the model and observed that the mass distribution of small and intermediate fragments obeys a power-law. The exponent of the power law, equal to $-3/2$, agrees fairly well with the reported experimental value. We show that this universal power-law dependence stretches up to the threshold fragment mass M_F and does not depend on the total

fragmentation energy E . We also conclude that this universal behavior is observed for the impact energy, smaller than the critical energy $E \leq E_{\text{crit}}$; in this case an incomplete fragmentation takes place and large fragments, with the mass of the order of the target mass exist. At the same time, for $E > E_{\text{crit}}$, which corresponds to the complete fragmentation regime, large fragments are lacking and an excess amount of small and intermediate fragments is present. The universal power-law distribution is distorted in this case. We have elaborated a scaling theory which allows to estimate the dependence of the threshold mass M_F on the total mass M and energy E and of the critical energy E_{crit} on the total mass.

We have developed an analytical theory which explains the nature of the power law in the fragmentation statistics and demonstrate that the proposed model gives a qualitative description for the overall fragment size distribution observed in experiments. From our results we find the statement made in the introduction confirmed that the physics of collisional aggregate fragmentation is largely dominated by a stochastic-statistical nature of the crack propagation.

Concerning future studies, first we plan to go beyond the scaling analysis and quantify the critical energy E_{crit} and the threshold mass M_F for adhesive–dissipative aggregates. These parameters depend crucially on the configuration (packing, porosity, dimension) of the aggregate and their knowledge allows to address the question, of how the mass-distribution function will change with the energy E for the case $E > E_{\text{crit}}$. Further, we want to extend the model to 3D adhesive aggregates—where one might think of a 2D random walk; here one has to assume constraints for the correlations between the two crack-tip directions.

Our final goal is to combine this rather simple fragmentation model with the coagulation of aggregates or constituents, in order to explain the mass (size) distribution of granular ice particles populating the dense planetary rings of Saturn which has been observed by certain space missions [29]. A far reaching goal is the application of the evolution of the size distribution of a cosmic granular gas to theories of planet formation, where an increasing number of detected extrasolar planets and surrounding dust discs provide a flood of new data waiting for their theoretical interpretation.

Acknowledgments

EVN and AHFG acknowledge support by the DAAD. EVN is grateful for the support by the grant FAPESP-2011/08171-3. FS gratefully thanks R Metzler for helpful discussions.

References

- [1] Grady D E and Lipkin J 1980 Criteria for impulsive rock fracture *Geophys. Res. Lett.* **7** 255–8
- [2] Turcotte D L 1997 *Fractals and Chaos in Geology and Geophysics* (Cambridge: Cambridge University Press)
- [3] Michel P, Benz W and Richardson D C 2003 Disruption of fragmented parent bodies as the origin of asteroid families *Nature* **421** 608–11
- [4] Nakamura A M *et al* 2008 Impact process of boulders on the surface of asteroid 25143 Itokawa—fragments from collisional disruption *Earth Planets Space* **60** 7–12 January
- [5] Thornton C, Yin K K and Adams M J 1996 Numerical simulation of the impact fracture and fragmentation of agglomerates *J. Phys. D: Appl. Phys.* **29** 424–35
- [6] Lankford J and Blanchard C R 1991 Fragmentation of brittle materials at high rates of loading *J. Mater. Sci.* **26** 3067–72
- [7] Mott N F and Linfoot E H 1943 *Technical Report AC 3384* Ministry of Supply
- [8] Grady D E 2006 *Fragmentation of Rings and Shells: The Legacy of N. F. Mott* (Berlin: Springer)

- [9] Herrmann H J and Roux S 1990 *Statistical Models for the Fracture of Disordered Media* (Amsterdam: Elsevier)
- [10] Nakamura A and Fujiwara A 1991 Velocity distribution of fragments formed in a simulated collisional disruption *Icarus* **92** 132–46
- [11] Giblin I, Martelli G, Farinella P, Paolicchi P, di Martino M and Smith P N 1998 The properties of fragments from catastrophic disruption events *Icarus* **134** 77–112
- [12] Arakawa M 1999 Collisional disruption of ice by high-velocity impact *Icarus* **142** 34–45
- [13] Ryan E V 2000 Asteroid fragmentation and evolution of asteroids *Annu. Rev. Earth Planet. Sci.* **28** 367–89
- [14] Herrmann H J, Wittel F K and Kun F 2006 Fragmentation *Physica A* **371** 59–66
- [15] Kun F, Wittel F K, Herrmann H J, Kröplin B H and Maloy K J 2006 Scaling behavior of fragment shapes *Phys. Rev. Lett.* **96** 025504
- [16] Güttler C, Blum J, Zsom A, Ormel C W and Dullemond C P 2010 The outcome of protoplanetary dust growth: pebbles, boulders, or planetesimals? I. Mapping the zoo of laboratory collision experiments *Astron. Astrophys.* **513** A56
- [17] Timar G, Blomer J, Kun F and Herrmann H J 2010 New universality class for the fragmentation of plastic materials *Phys. Rev. Lett.* **104** 095502
- [18] Astrom J A, Ouchterlony F, Linna J and Timonen R P 2004 Universal dynamic fragmentation in D dimensions *Phys. Rev. Lett.* **92** 245506
- [19] Grady D E 2009 Length scales and size distributions in dynamic fragmentation *Int. J. Fract.* **163** 85–99
- [20] Chang C S, Wang T K, Sluys L J and van Mier J G M 2002 Fracture modeling using a micro-structural mechanics approach: II. Finite element analysis *Eng. Fract. Mech.* **69** 1959–76
- [21] Benz W and Asphaug E 1994 Impact simulations with fracture: I. Method and tests *Icarus* **107** 98–116
- [22] Bouchaud J P, Bouchaud E, Lapasset G and Planès J 1993 Models of fractal cracks *Phys. Rev. Lett.* **71** 2240–3
- [23] Galybin A N and Dyskin A V 2004 Random trajectories of crack growth caused by spatial stress fluctuations *Int. J. Fract.* **128** 95–103
- [24] Paolicchi P, Verlicchi A and Cellino A 1996 An improved semi-empirical model of catastrophic impact processes: I. Theory and laboratory experiments *Icarus* **121** 126–57
- [25] Chang C S, Wang T K, Sluys L J and van Mier J G M 2002 Fracture modeling using a micro-structural mechanics approach—I. Theory and formulation *Eng. Fract. Mech.* **69** 1941–58
- [26] Kun F and Herrmann H J 1999 Transition from damage to fragmentation in collision of solids *Phys. Rev. E* **59** 2623–32
- [27] Longaretti P-Y 1989 Saturn's main ring particle size distribution: an analytic approach *Icarus* **81** 51–73
- [28] Spahn F, Albers N, Sremcevic M and Thornton C 2004 Kinetic description of coagulation and fragmentation in dilute granular particle ensembles *Europhys. Lett.* **67** 545–51
- [29] Sremčević M, Schmidt J, Salo H, Seiß M, Spahn F and Albers N 2007 A belt of moonlets in Saturn's a ring *Nature* **449** 1019–21
- [30] Dullemond C P and Dominik C 2005 Dust coagulation in protoplanetary disks: a rapid depletion of small grains *Astron. Astrophys.* **434** 971–86
- [31] Ormel C W, Spaans M and Tielens A G G M 2007 Dust coagulation in protoplanetary disks: porosity matters *Astron. Astrophys.* **461** 215–32
- [32] Brauer F, Dullemond C P and Henning T 2008 Coagulation, fragmentation and radial motion of solid particles in protoplanetary disks *Astron. Astrophys.* **480** 859–77
- [33] Guimarães A H F, Albers N, Spahn F, Seiß M, Vieira-Neto E and Brilliantov N V 2012 Aggregates in the strength and gravity regime: particles sizes in Saturn's rings *Icarus* **220** 660–78
- [34] Brilliantov N, Albers N, Spahn F and Poeschel T 2007 Collision dynamics of granular particles with adhesion *Phys. Rev. E* **76** 051302
- [35] Redner S and Krapivsky P L 1999 Capture of the lamb: diffusing predators seeking a diffusing prey *Am. J. Phys.* **67** 1277–83
- [36] Krapivsky P L, Redner S and Ben-Naim E 2010 *A Kinetic View of Statistical Physics* (Cambridge: Cambridge University Press)